Integrated Optical Switch Matrix for Single-Mode Fiber Networks

MICHIKAZU KONDO, YOSHINORI OHTA, MASAHIKO FUJIWARA, AND MITSUHITO SAKAGUCHI

Abstract—**Design analysis and experiments on optical directional coupler switch integration into an $LiNbO_3$ chip with arrayed fiber pigtails has been made at 1.3 μm wavelength. A limitation for high integration was discussed by taking into account radiation losses at connecting waveguides between switch elements and at the input/output curved waveguide, switching voltage, and crosstalk caused by applied electric field leakage. An optimum designed low-loss 4 × 4 switch matrix with arrayed fiber pigtails at 1.3 μm wavelength has been developed. Its insertion loss was measured to be as low as 6 dB.**

I. Introduction

SINGLE-MODE optical fiber communication systems have a very large transmission capacity in the long wavelength region [1] because fiber group velocity dispersion is minimum at 1.3 μm [2]. Additionally, fiber transmission loss is low [3]. For these systems, high-speed switching networks are very attractive for attaining a variety of functions, for example, space-division optical switching [4] for analog or digital signals, and optical sampling in multiplexer and time-division switching.

Integrating guided wave switches [5]-[8] is an effective way to realize such switching networks because of high switching speed, adaptability to single-mode fiber systems, and integration ease. The guided wave switches have particular features, i.e., optical signal frequency is not limited because they are transmitted without any conversion to electric signal, and it is easy to switch bidirectional optical signals. In optoelectronic switches [9] with O/E and E/O conversion, the optical signal frequency is limited by the electric circuit high-frequency cutoff, and a complicated electric circuit is required for bidirectional switching. A variety of guided wave switches has been developed with dielectric and semiconducting materials. In particular, $LiNbO_3$ electrooptic switches [10] have excellent features, i.e., low drive voltage compared to other kinds of switches because of large electrooptic coefficients, low-loss characteristics, and fabrication ease using Ti diffusion. There are several structures pertinent to constructing optical switch elements in $LiNbO_3$ crystal. They are the directional coupler switch [11], the total internal reflecting (TIR) switch [12], the Bragg deflecting switch, [7] and the balanced bridge interferometric switch [13]. Switching voltage and crosstalk are important parameters for switch performance as well as optical insertion loss. Several design considerations for optimum switch structures have been made and almost good enough level performances, for example, -26 dB crosstalk [14] and 3 V switching voltage [15] in directional coupler switches, have been obtained as single switch elements. However, to obtain high-speed switching networks in optical communication systems with large capacity, multichannel switches connected to single-mode fiber arrays with low insertion loss must be realized in the 1.3 μm wavelength region. For such purposes, few considerations have been made.

Matrix switches with five directional coupler switch elements [5] or five TIR switch elements [18] have been demonstrated at 0.6328 μm, without coupling to fibers, and a 2 × 2 directional coupler switch with fiber pigtails has been demonstrated at 0.83 μm [16]. However, these switches cannot satisfy the above-mentioned multichannel switch conditions. A low-loss optical circuit design is required for switch element integration to interconnect between switch elements and between switch elements and fibers.

This paper describes design considerations on the matrix switch waveguide and experimental results obtained from a low optical loss and a low drive voltage 4 × 4 matrix switch with 1.3 μm single-mode fiber arrayed pigtails. The matrix switch discussed here is constructed by a tandem combination of directional coupler switch elements, which are used as 2 × 2 switches, as shown in Fig. 1. A directional coupler switch is suitable for constructing a matrix switch because of the simple structure, low switching voltage, and low crosstalk relative to other kinds of switches. This matrix switch is composed of 2 × 2 switch elements, connecting waveguides between switch elements, and input/output curved waveguides leading to optical fiber arrays. In this arrangement, two important problems arise, which need not be considered in constructing a single switch or without connecting to fiber arrays. They are

1) increase in transmission loss at connecting waveguides and input/output waveguides, and increase in operating voltage due to reducing individual waveguide lengths for one chip integration, and

2) applied electric field interference effect between closed switch elements.

Increases in loss and drive voltage caused by minimizing the optical circuit are estimated in Section II, and interference effects are discussed in Section III. From these considerations, the required dimensions for highly integrated switches are discussed in Section IV. Section V describes experimental results obtained from a low-loss 4 × 4 switch with single-mode fiber arrayed pigtails, which has been fabricated to conform to the above considerations.

Manuscript received February 26, 1982; revised June 8, 1982.

The authors are with Opto-Electronics Research Laboratories, Nippon Electric Company, Ltd., Takatsu-ku, Kawasaki 213, Japan.

0018-9480/82/1000-1747$00.75

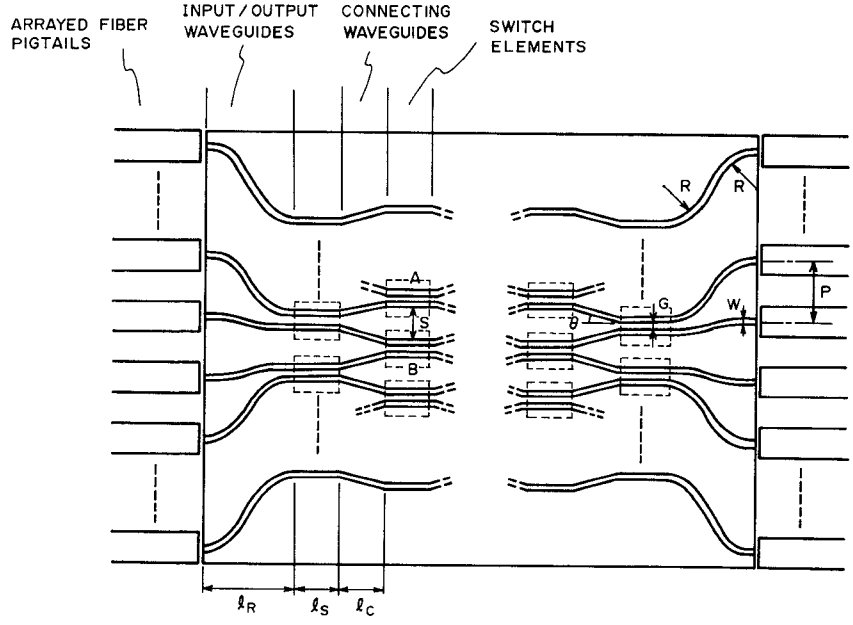

Fig. 1. Optical waveguide matrix switch with arrayed fiber pigtails, composed of 2 X 2 directional coupler switch elements, connecting waveguides between the switch elements and input/output curved waveguides.

II. Problems on Small Size Optical Circuit

To obtain a highly integrated optical switch circuit fabricated on one chip, as shown in Fig. 1, individual parts must have as short a length as possible. As lengths become shorter, radiation loss in input/output waveguides and connecting waveguides increases because of abrupt directional change, and the switch element drive voltage increases. In this section, these effects are discussed for the 10 μm waveguide width because fibers with a 10 μm core diameter and a 125 μm cladding diameter are very frequently used in the 1.3 μm wavelength region. The switching circuit waveguide width is matched to the 10 μm core diameter for low-loss coupling [16], [17].

First, consider the input/output waveguide loss increase. Input/output waveguide spacing must be larger than fiber diameter at the waveguide facets. On the other hand, waveguides at switch elements are close to each other. Therefore, curved waveguides are necessary to connect switch elements with arrayed optical fibers, as shown in Fig. 1. Fig. 2 shows the required input/output waveguide lengths l_R versus the outermost waveguide curvature R, provided that the spacing between switch elements is 30 μm and the fiber diameters are 125 μm. Here, the 30 μm switch spacing is required to reduce the interference effect, as discussed later. The total offset in the transverse direction between the opposite ends of section l_R is 154 and 348 μm for 4 X 4 and 8 X 8 switches, respectively. To obtain short waveguides length l_R, curvature R must be small. Then, radiation loss α_R at the curved waveguides increases. Radiation loss α_R had been calculated theoretically for the step index profile waveguide by Neumann *et al.* [18], and is given approximately as

$$\alpha_R = A(n \cdot \Delta n/\lambda) \exp\{-B(n \cdot \Delta n)^{3/2}/\lambda\} \cdots \quad (1)$$

where n is the waveguide refractive index, Δn is the effective refractive index difference between substrate and waveguides, λ is the optical wavelength in free space, and A and B are constants. A and B had been determined in the theory for step index waveguides. However, with these values, the calculated α_R curve is different from $LiNbO_3$:Ti-diffused waveguide experimental data. Here, values A and B were determined using experimental data at 0.6328 Å to make α_R rough estimation at 1.3 μm. Fig. 3 shows measured α_R data and estimated α_R curves versus Δn. As $LiNbO_3$ Ti-diffused waveguides usually have $\Delta n \geq 2 \times 10^{-3}$ [19], $R \geq 30$ mm is required for obtaining $\alpha_R \leq 1$ dB/cm in this Δn region. From Fig. 2, the minimum input/output waveguide length l_R is about 4.2 mm for a 4 X 4 switch and 6.4 mm for an 8 X 8 switch in this low-loss waveguide condition.

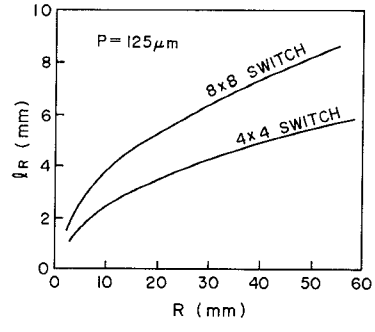

Fig. 2. Input/output waveguides length l_R versus waveguide curvature R required in a 4 X 4 or an 8 X 8 matrix switch connected with 125 μm diameter optical fiber arrays, provided that switch element spacings are 30 μm.

The second problem is radiation loss increase due to the tandem connection of many switch elements. To separate neighboring switch elements, for example, elements A and B in Fig. 1, connecting waveguides have an S-shaped bend made of three straight waveguides connected at angle θ. The required

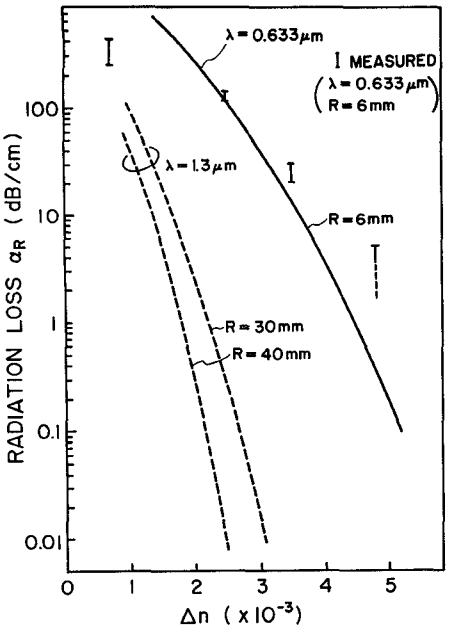

Fig. 3. Radiation loss α_R versus effective refractive index difference Δn between substrate and waveguide in the curved waveguide. Dotted line shows estimated curves at 1.3 μm by modification of theoretical curves using measured α_R data in a Ti-diffused waveguide at 0.6328 μm.

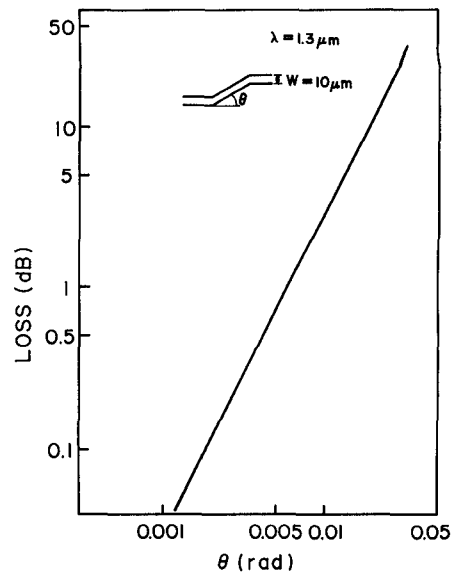

Fig. 4. Calculated radiation loss α at the 1.3 μm wavelength versus directional changing angle θ in the S-shaped waveguide composed of three straight waveguides with 10 μm widths by the method in [20].

spacings between the two switch elements must be larger than the 30 μm separating distance, which will be explained later. If the connecting waveguide length l_C is short, the angle θ must be large, and radiation losses caused by directional change increase according to θ. For the S-shaped bend waveguide with a 10 μm width and sharp corners, loss α at 1.3 μm is calculated according to [20], as shown in Fig. 4. For loss $\alpha \leqslant 0.5$ dB, angle θ must be less than 4.5 mrad, and length l_c required for the 30 μm spacing is larger than about 3 mm. The minimum connecting waveguides total length is 9 mm for a 4 X 4 switch with a four-stage switch tandem connection and 21 mm for an 8 X 8 switch with an eight-stage switch tandem connection.

The third problem is increase in switch drive voltage. Here, several conditions are provided to facilitate the switching voltage estimation. The first condition is that complete coupling length L_c, equal to switch element length l_s, and uniform electrodes with the same width as waveguides are placed on both waveguides. The switching voltage obtained from this condition is a little higher than the minimum switching voltage required in the stepped $\Delta\beta$ reversal driving by about 10 percent [21]. The second condition is that the phase mismatch $\Delta\beta$ is directly caused by the induced electric field at the center of the optical guided wave field, which is about 3-4 μm deep from the surface in a diffusion condition which gives waveguide to fiber low-loss coupling [17]. To obtain the strict switching voltage, the phase constant deviation in the waveguide with a refractive index distribution change caused by induced electric field must be calculated. The third condition is that gap G in the two waveguides, with 10 μm widths, is 4 μm, which can be reasonable to effectively induce the deep electric field mentioned above.

Under these conditions, the switch is in the crossover (⊗) state without applied voltage and turns to the straight-through (⊜) state when voltage V is applied, where V is given by (2) for TM operation in Z-cut $LiNbO_3$ substrate [11].

$$\delta n = (\sqrt{3}/4)\,\lambda/L_c = \tfrac{1}{2} n^3 r_{33} \eta \{V/(G+W)\} \cdots. \quad (2)$$

Here, δn is the effective refractive index change, which is induced by the electrooptic effect and gives $\Delta\beta$ required for this switching, r_{33} is the electrooptic coefficient, and η is a constant which is a ratio of the electric field amplitude induced in the waveguides to that induced by two parallel electrodes placed the same distance $(G + W)$ away as the waveguide centers. In this case, with $W = 10$ μm, $G = 4$ μm, and a 4 μm electric field depth, η was determined to be 0.56 by the electric field distribution calculated using the successive over-relaxation (SOR) method [22]. Fig. 5 shows the calculated switching voltage versus the switch element length l_s. At a high switching speed of more than several tens of megahertz, high drive voltage causes high power dissipation in the drive circuit. However, less than 5 V switching voltage for transistor-transistor logic (TTL) driving requires as much as 15 mm of switch element length, by which only one or two switch elements can be integrated on a chip. If less than 15 V are desired for the multichannel switch, the minimum element length is 5.8 mm.

III. Interference Effect Between Switch Elements

When switch elements are placed with narrow spacings between them, optical power coupling and applied electric field leakage must be considered. Optical crosstalk δ_0, caused by optical power coupling between switch elements separated by distance S, can be calculated as shown in Fig. 6 (dotted line) by the modified Wentzel-Kramer-Brillouin (WKB) approximation method reported by Noda *et al.* [23]. Here, the 10 μm waveguide width, the 3.3 μm lateral diffusion depth, and $\Delta n_{\text{eff}} = 2 \times 10^{-3}$ are provided as typical conditions. Optical crosstalk δ_0 is small, less than -30 dB with $S \geqslant 15$ μm.

However, when voltage is applied on an element, the induced electric field distributes over a wide region. Fig. 7 shows a side

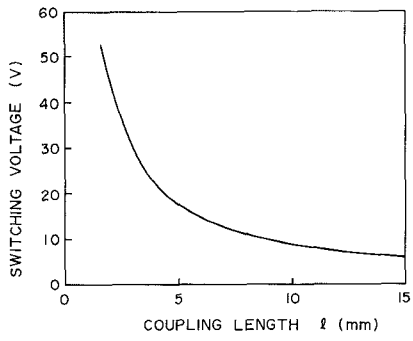

Fig. 5. Calculated switching voltage versus switch element length l_S. Uniform electrodes are placed on two 10 μm wide waveguides separated by 4 μm in a Z-cut $LiNbO_3$ and $l_S = L_C$, and the optical guided wave field is 3–4 μm deep from the surface.

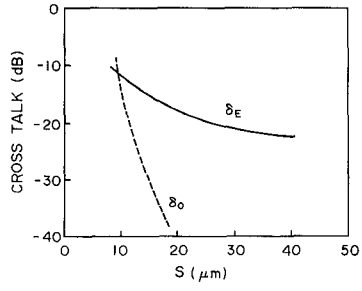

Fig. 6. Optical crosstalk caused by interference effect versus switch element spacing S. Dotted line indicates the crosstalk by optical power coupling between switch elements, and solid line indicates the crosstalk caused by switching state deviation in an element due to applied electric field leakage.

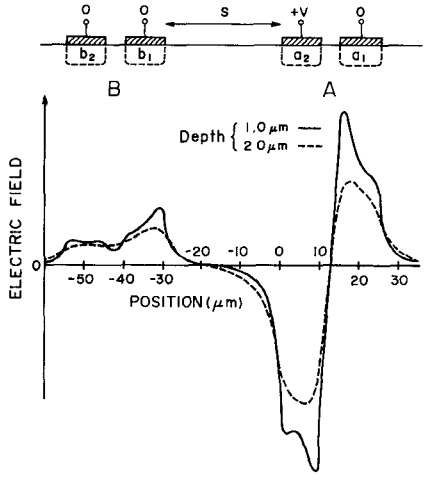

Fig. 7. Side view of two neighboring switch elements A and B separated by $S = 30$ μm. Calculated electric field distribution when voltage is applied on only an electrode in element A.

view of two neighboring switch elements A and B, separated from each other by $S = 30$ μm, and calculated electric field distribution by the SOR method when voltage V is applied on an electrode in element A. In Fig. 7, a weak leak electric field was generated in two waveguides making up element B asymmetrically. If the switch elements are designed as the ⊗ state without applied voltage and the ⊖ state with applied voltage V, the leak electric field in element B causes deviation from the ⊗ state and results in optical crosstalk δ_E, which is given by (3):

$$\delta_E = 1 - \{1/(1+3\gamma^2)\} \sin^2 \{(\pi/2)\sqrt{1+3\gamma^2}\} \cdots. \quad (3)$$

Here, $\gamma = \Delta E/E_0$ where E_0 is the applied electric field difference between element A waveguides and ΔE is the leak electric field difference between element B waveguides. The solid line in Fig. 6 shows the calculated optical crosstalk δ_E value versus spacing S under the above conditions. Here, E_0 and ΔE were determined by the electric field at the center of the optical guided wave field. Spacing $S \geqslant 30$ μm is required to obtain $\delta_E \leqslant -21$ dB. This minimum spacing limits connecting waveguide length l_c, as mentioned in Section II.

IV. Matrix Switch Dimension

The results obtained in the discussions of Sections II and III give a limitation on integrated matrix switch dimension with low loss, low drive voltage, and little interference effect connected with arrayed fibers. For example, an optimally designed 8 X 8 matrix switch, with an eight-stage directional coupler switch tandem connection along the optical path, is desired to have a 12.8 mm total input/output waveguide length, a 21 mm total interconnecting waveguide length, and a 46.4 mm total switch element length. As a result, the total device length becomes as great as 80 mm. Therefore, some new techniques are required to realize such high level integration as an 8 X 8 switch on an available $LiNbO_3$ chip to reduce waveguide lengths without increasing losses, drive voltages, and interference effects. One of these techniques is thick titanium diffusion at the curved waveguides, obtaining a large refractive index difference, and as a result, low radiation losses. This method was confirmed by an experiment on a directional coupler switch with input/output curved waveguides connected to fibers at the 0.63 μm wavelength. The switch parameters had a 3 μm waveguide width, a 3 μm separation between two waveguides in the directional coupler, and a 6 mm input/output waveguide curvature. Titanium thickness was optimized in the switch element and the curved waveguides individually, so that both pertinent complete coupling length and low radiation loss could be obtained. In this case, radiation loss was reduced by 20 dB compared to the case of uniform Ti thickness optimized in the switch element. To obtain a shorter switch element length and a shorter interconnecting waveguide length, the electric field applied on one switch element mut be more confined, attaining lower drive voltage and less electric field leakage.

On the other hand, a 4 X 4 matrix switch with a four-stage switch element tandem connection can be fabricated on one chip using a conventional technique because the desired total length is about 40 mm, according to similar considerations.

V. 4 X 4 Switch with Single-Mode Fiber Arrayed Pigtails

To confirm the above consideration, a 4 X 4 switch matrix was fabricated with single-mode arrayed fiber pigtails. Five directional coupler switch elements are integrated on a Z-cut $LiNbO_3$ chip as shown in Fig. 8. Here, a three-stage switch element tandem connection was selected for obtaining lower loss and lower switching voltage. Optical switch circuits are designed optimally at 1.3 μm. Switch circuit parameters are $R = 40$ mm, $l_R = 5$ mm, $\theta = 4.5$ mrad, $l_c = 3$ mm,

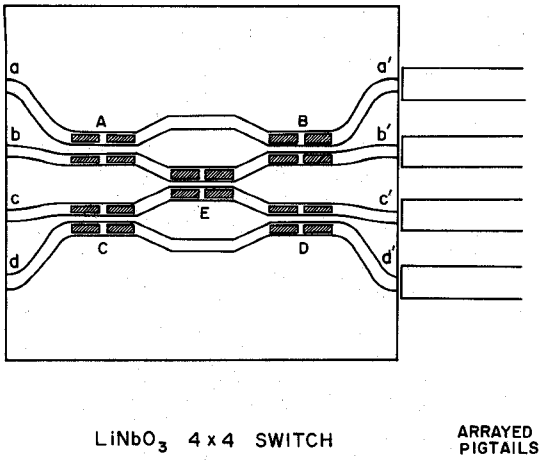

Fig. 8. Fabricated $LiNbO_3$ 4 × 4 switch configuration with arrayed fiber pigtails.

$S = 30\ \mu m$, $l_s = 8$ mm, $W = 10\ \mu m$, $G = 4\ \mu m$, and the total waveguide length is 40 mm. The spacing between input/output waveguides is 125 μm. A 480 Å thick Ti waveguides pattern was diffused at 1040°C for 8 h. This diffusion process was accomplished in air flow, and no out-diffused modes were observed. After the diffusion process, a 2000 Å thick SiO_2 optical buffer layer was deposited over the waveguides. Aluminum electrodes were made on each switch element guide for $\Delta\beta$ reversal driving. Here, waveguide width W and diffusion parameters were optimized in order to obtain low-loss coupling in the optical fiber field with the guided wave field. Waveguide gap G at switch elements was selected to satisfy the two-section $\Delta\beta$ reversal driving condition, i.e., $1 \leqslant l_s/L_c \leqslant 3$.

First, optical transmission characteristics were measured by a rutile prism coupler with a 1.3 μm wavelength laser diode. Total output optical power from four waveguides through the prism was plotted along the optical path as shown in Fig. 9. Output level dip at position x = 5–10 mm is due to the incomplete prism contact. The propagation loss estimated from Fig. 9 by taking into account the ±0.5 dB accuracy of the measurement is below 0.3 dB/cm, which is less than the values reported with shorter wavelength, indicating that radiation loss at curved waveguides and interconnecting loss between switch elements are very small, in agreement with designed values. Complete coupling length L_c was measured to be 5–6 mm, satisfying the $\Delta\beta$ reversal switching condition.

An input single-mode fiber about 1 m long is connected to the end facet of one of the waveguides. A 1.3 μm wavelength laser diode was coupled to the other end facet of the input fiber by small lenses. A single-mode fiber array with four fibers, which were sandwiched between two silicon chips with V grooves [24], was connected to the output end facet of the switch. The input fiber and the output arrayed fiber pigtails were fixed to the switch mount by epoxy adhesive. Fig. 10 shows the fiber pigtailed 4 × 4 switch and the experimental arrangement. Total insertion loss, which is a ratio of the optical power which emerged from the four output fibers to that which emerged from the input fiber without applying any voltage, was measured to be 6.25 dB. This loss can be divided, as shown in Table I. The output fiber array coupling loss is larger than the input fiber coupling loss by about 1 dB, due to the spacing deviation between the arrayed fibers. The epoxy

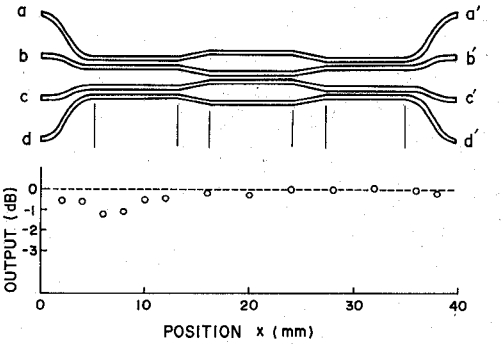

Fig. 9. Total output optical power from the four waveguides through the prism measured along the optical path.

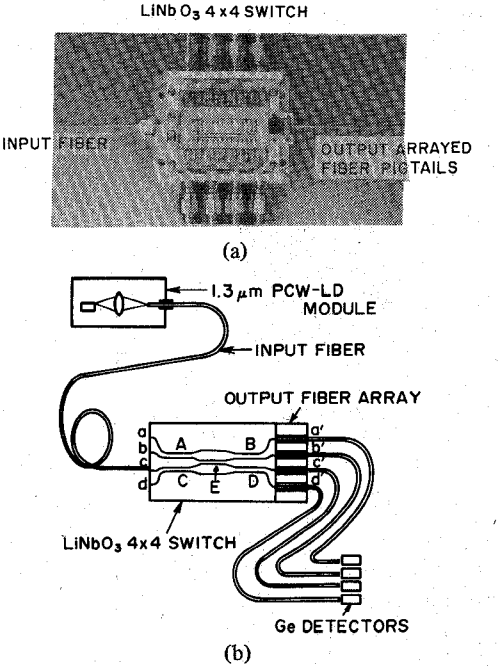

Fig. 10. (a) Fiber pigtailed 4 × 4 switch. (b) Experimental arrangement.

TABLE I
CLASSIFICATION OF THE INSERTION LOSS

Waveguide propagation loss	1.2 ± 0.2 dB
Input fiber coupling loss	1.2 ± 0.2
Output fiber array coupling loss	2.2
Reflection loss at $LiNbO_3$ facets	1.3
Reflection loss at output fiber facets	0.35
Total insertion loss	6.25 dB

adhesive between the silicon V grooves was too thick to arrange the fibers precisely. Fig. 11 shows switching characteristics, indicating variation in optical intensity from the two output ports of a switch element versus applied voltage with $\Delta\beta$ reversal driving. The crossover state and straight-through state voltages are 12 and 28 V, respectively, which are a little higher than the 9.5 and 23.4 V values foreseen by a similar estimation described in Section II, respectively. In uniform $\Delta\beta$ driving, the straight-through state is obtained at 9 V. Each switch

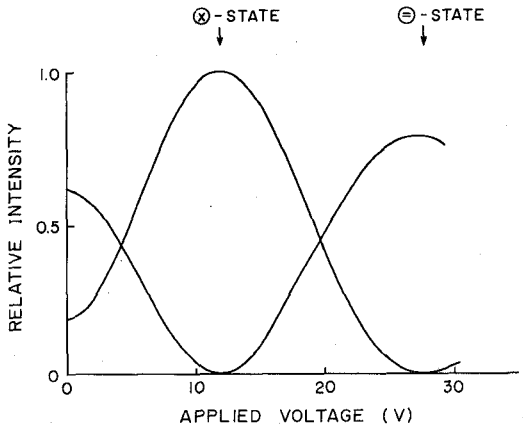

Fig. 11. Switching characteristics for one element by $\Delta\beta$ reversal driving. The crossover state and straight-through state are 12 and 28 V, respectively.

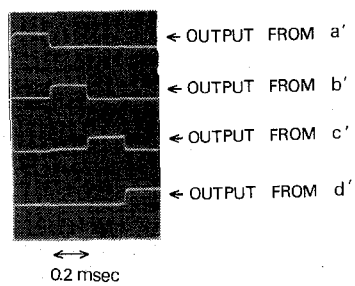

Fig. 12. Light signals from four output fibers. Input light coupled to waveguide *C* is switched periodically.

element optical crosstalk was measured to be less than −18 dB for both ⊗ and ⊖ states. Five switching elements have almost the same switching characteristics. Incident light could be switched into any of the four output fibers by pertinently driving each switch element. Fig. 12 shows the light signals detected at each output fiber when input light at waveguide *C* is switched periodically. In this case, total throughput crosstalk is less than −14 dB. Output level variation among four fibers was ±0.7 dB, which is due to the spacing variation of the arrayed fibers mentioned above. Optical power in waveguides was about 1.0 mW. No optical damage was observed in experiments at this wavelength.

VI. Conclusion

Design considerations and experiments on directional coupler switch integration have been made for constructing switching networks in the single-mode fiber communication systems at 1.3 μm. Integration of a large number of optical switch elements in a chip brings about excessive loss, high drive voltage, and optical crosstalk by interference effects between switch elements. To obtain an 8 × 8 optical matrix switch with high performance on an available chip, each waveguide titanium thickness must be selected individually for reducing waveguide lengths without increasing loss, and a technique for confining an electric field in one switch element is required. A 4 × 4 optical switch circuit can be constructed on an available 2 in diameter $LiNbO_3$ chip by optimum design, being almost free from the above problems. This integrated-optical switching circuit design consideration was confirmed by experimental results from a low-loss 4 × 4 switch matrix with arrayed single-mode fiber pigtails at 1.3 μm. This switch has a 6.25 dB insertion loss, including as much as about a 1.2 dB waveguide transmission loss.

Acknowledgment

The authors would like to thank Dr. T. Uchida and Dr. F. Saito of the Opto-Electronics Research Laboratories, Nippon Electric Company, Ltd., for their continuous guidance and encouragement.

References

[1] J. Yamada, S. Machida, and T. Kimura, "2G bit/s optical transmission experiments at 1.3 μm with 44 km single-mode fibre," *Electron. Lett.*, vol. 17, pp. 479–480, June 1981.

[2] D. E. Payne and W. A. Gambling, "Zero material dispersion in optical fibers," *Electron. Lett.*, vol. 11, pp. 176–178, Apr. 1975.

[3] T. Moriyama, O. Fukuda, K. Sanada, K. Inada, T. Edahiro, and K. Chida, "Ultimately low OH content V.A.D. optical fibers," *Electron. Lett.*, vol. 16, pp. 698–699, Aug. 1980.

[4] J. Minowa, Y. Fujii, Y. Nagata, T. Aoyama, and K. Doi, "Nonblocking 8 × 8 optical matrix switch for fiber-optic communication," *Electron. Lett.*, vol. 16, pp. 422–423, May 1980.

[5] R. V. Schmidt and L. L. Buhl, "Experimental 4 × 4 optical switching network," *Electron. Lett.*, vol. 12, pp. 575–577, Oct. 1976.

[6] J. C. Shelton, F. R. Reinhart, and R. A. Logan, "Single-mode GaAs–$Al_xGa_{1-x}As$ rib waveguide switches," *Appl. Opt.*, vol. 17, pp. 890–891, Mar. 1978.

[7] R. A. Becker and W.S.C. Chang, "Electrooptical switching in thin film waveguides for a computer communication bus," *Appl. Opt.*, vol. 18, pp. 3296–3300, Oct. 1979.

[8] C. L. Chang, F. R. El-Akkari, and C. S. Tsai, "Fabrication and testing of optical channel waveguide total internal reflection (TIR) switching networks," *Soc. Photoopt. Instrum. Eng., Guided-Wave Optical and Surface Acoustic Wave Devices, Systems, and Applications*, vol. 239, July 1980.

[9] R. I. MacDonald and E. H. Hara, "Switching with photodiodes," *IEEE J. Quantum Electron.*, vol. QE-16, pp. 289–295, Mar. 1980.

[10] R. C. Alferness, "Guided-wave devices for optical communication," *IEEE J. Quantum Electron.*, vol. QE-17, pp. 946–958, June 1981.

[11] R. V. Schmidt and R. C. Alferness, "Directional coupler switches, modulators, and filters using alternating $\Delta\beta$ techniques," *IEEE Trans. Circuits Syst.*, vol. CAS-26, pp. 1099–1108, Dec. 1979.

[12] F. R. El-Akkari, C. L. Chang, and C. S. Tsai, "Electrooptical channel waveguide matrix switch using total internal reflection," presented at the Topical Meet., Integrated Guided-Wave Opt., Incline Village, NV, Jan. 1980, paper TuE4.

[13] O. Mikami and S. Zembutsu, "Modified balanced-bridge switch with two straight waveguides," *Appl. Phys. Lett.*, vol. 35, pp. 145–147, July 1979.

[14] R. V. Schmidt and H. Kogelink, "Electro-optically switched coupler with stepped $\Delta\beta$ reversal using Ti-diffused $LiNbO_3$ waveguides," *Appl. Phys. Lett.*, vol. 28, pp. 503–506, May 1976.

[15] R. V. Schmidt and P. S. Cross, "Efficient optical waveguides switch/amplitude modulator," *Opt. Lett.*, vol. 2, pp. 45–47, Feb. 1978.

[16] O. G. Ramer, C. Nelson, and C. Mohr, "Experimental integrated optic circuit losses and fiber pigtailing of chips," *IEEE J. Quantum Electron.*, vol. QE-17, pp. 970–974, June 1981.

[17] M. Fukuma and J. Noda, "Optical properties of Ti-diffused $LiNbO_3$ strip waveguides and their coupling-to-a fiber characteristics," *Appl. Opt.*, vol. 19, pp. 591–597, Feb. 1980.

[18] E. G. Neumann and H. D. Rudolph, "Radiation from bends in dielectric rod transmission lines," *IEEE Trans. Microwave Theory Tech.*, vol. MTT-23, pp. 142–149, Jan. 1975.

[19] M. Minakata, S. Saito, M. Shibata, and S. Miyazawa, "Precise determination of refractive-index changes in Ti-diffused $LiNbO_3$ optical waveguides," *J. Appl. Phys.*, vol. 49, pp. 4677–4682, Sept. 1978.

[20] L. D. Hutcheson, I. A. White, and J. J. Burke, "Comparison of bending losses in integrated optical circuits," *Opt. Lett.*, vol. 5, pp. 276–278, June 1980.

[21] H. Kogelnik and R. V. Schmidt, "Switched directional couplers with alternating $\Delta\beta$," *IEEE J. Quantum Electron.*, vol. QE-12, pp. 396–401, July 1976.

[22] H. E. Green, "The numerical solution of some important transmission-line problems," *IEEE Trans. Microwave Theory Tech.*, vol. MTT-13, pp. 676–692, Sept. 1965.

[23] J. Noda, M. Fukuma, and O. Mikami, "Design calculation for directional couplers fabricated by Ti-diffused $LiNbO_3$ waveguides," *Appl. Opt.*, vol. 20, pp. 2284–2290, July 1981.
[24] C. M. Schroder, "Accurate silicon space chips for an optical-fiber cable connector," *Bell Syst. Tech. J.*, vol. 57, pp. 91–97, Jan. 1978.

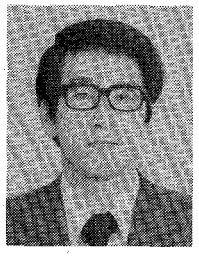

Michikazu Kondo was born in Shizuoka, Japan, on December 17, 1947. He received the B.S. and M.S. degrees in electronic engineering from Shizuoka University, Shizuoka, Japan, in 1970 and 1972, respectively.

He joined Nippon Electric Company, Ltd., Kawasaki, Japan, in 1972, and has been engaged in the research and development of electrooptic modulators, switches, and guided wave optical devices.

Mr. Kondo is a member of the Institute of Electronics and Communication Engineers of Japan and the Japan Society of Applied Physics.

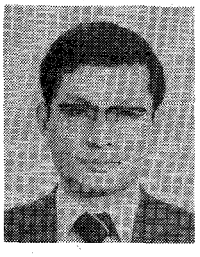

Yoshinori Ohta was born on March 10, 1945. He received the B.S. and M.S. degrees in telecommunication engineering from Tohoku University, Sendai, Japan, in 1968 and 1970, respectively.

He joined Nippon Electric Company, Ltd., Kawasaki, Japan, in 1970, and is now a Supervisor of the Opto-Electronics Research Laboratories. He is engaged in the research and development of electrooptic devices for fiber optical transmission systems.

Mr. Ohta is a member of the Institute of Electronics and Communication Engineers of Japan and the Japan Society of Applied Physics.

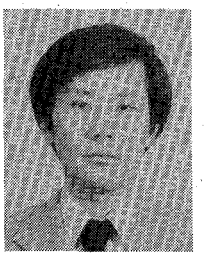

Masahiko Fujiwara was born in Tokyo, Japan, on February 18, 1953. He received the B.S. and M.S. degrees in electrical engineering from Yokohama National University, Kanagawa, Japan, in 1975 and 1977, respectively.

In 1977 he joined the Nippon Electric Company, Ltd., Kawasaki, Japan, where he has been engaged in the research and development of laser diode application and integrated optics.

Mr. Fujiwara is a member of the Institute of Electronics and Communication Engineers of Japan and the Japan Society of Applied Physics.

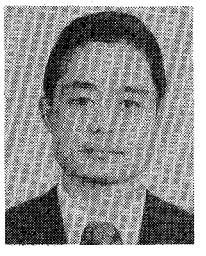

Mitsuhito Sakaguchi was born in Matsusaka, Mie, Japan, on February 5, 1940. He received the B.S. degree in electrical engineering from Nagoya Institute of Technology, Nagoya, Japan, in 1962 and the Ph.D. degree in engineering from Osaka University, Osaka, Japan, in 1978.

In 1962 he joined Nippon Electric Company, Ltd., Kawasaki, Japan, and is now Manager of the Opto-Electronic Application Research Laboratory in the Opto-Electronics Research Laboratories.

Dr. Sakaguchi is a member of the Institute of Electronics and Communication Engineers of Japan and the Japan Society of Applied Physics.

Measurement and Analysis of Periodic Coupling in Silicon-Clad Planar Waveguides

GLEN M. MC WRIGHT, STUDENT MEMBER, IEEE, T. E. BATCHMAN, MEMBER, IEEE, AND M. S. STANZIANO, STUDENT MEMBER, IEEE

Abstract—**Computer modeling studies indicate that planar dielectric waveguides clad with silicon exhibit a damped periodic oscillation in their attenuation and phase characteristics. The effect is due to a periodic coupling between the lossy, guided modes in the silicon film and the TE_0 mode of the dielectric waveguide. Experimental confirmation of the periodic coupling for a wavelength of 632.8 nm is presented. Propagation characteristics for a wavelength of 1150 nm were investigated for application in integrated optical modulators. Frequency filtering properties of silicon-clad waveguides are also examined and it is shown that the silicon thickness controls the filter response curve.**

Manuscript received March 1, 1982; revised May 13, 1982. This work was supported by the NASA Langely Research Center.

The authors are with the Department of Electrical Engineering, University of Virginia, Charlottesville, VA 22901.

I. Introduction

METAL-clad optical waveguides have been studied extensively and have found considerable application in electrooptic and magnetooptic modulators [1]–[5]. Semiconductor-clad or positive permittivity metal-clad waveguides are characterized by high attenuations which have severely limited their application, although they may be useful as cutoff polarizers or attenuators [6], and more recently, for optical control of millimeter wave propagation [7], [8]. We discuss further applications for these semiconductor-clad waveguides [9] and report, in this paper, the experimental confirmation of the predicted characteristics. Frequency filtering is also suggested as an application for these clad guides in the optical propagation region based on predictions presented here.

0018-9480/82/1000-1753$00.75